

ZnO Nanocrystals: Surprisingly ‘Alive’

Moazzam Ali and Markus Winterer*

*Nanoparticle Process Technology and Center for Nanointegration Duisburg-Essen (CeNide), University
Duisburg-Essen, Duisburg 47057, Germany*

Received July 22, 2009. Revised Manuscript Received September 8, 2009

In the past few years, ZnO has become one of the most elaborately and extensively studied nanocrystalline material. It is often assumed that ZnO nanomaterials are stable in ambient atmosphere. Contrary to this general—but not fully substantiated—belief we show that ZnO nanocrystals in *powder* form grow unexpectedly in ambient atmosphere at room temperature and the growth is influenced by the vapor pressure of water. Growth kinetics and mechanism, based on chemisorption of water on the surface of ZnO nanocrystals, are proposed. Water vapor not only causes the ZnO nanocrystals to grow but it also improves the crystallinity of the material. This unusual self-healing behavior of ZnO nanocrystals can remarkably influence their properties and affect their numerous applications.

Introduction

Over the past decade, the interest in ZnO nanomaterials has increased dramatically. The larger surface to volume ratio of nanocrystalline ZnO makes it a good candidate for gas sensing as well as heterogeneous catalysis.^{1,2} ZnO is a wide band gap (3.37 eV) semiconductor, which makes it a suitable candidate for ultraviolet LEDs and lasers.³ The high exciton binding energy (60 meV) of ZnO makes it a highly efficient laser-material, operable at room temperature.³ The low absorbance of visible light and improved conductivity after doping, puts ZnO in the category of the best transparent conducting materials.⁴ Size-reduction of ZnO into the nanoregime generates novel optical, electrical, mechanical and chemical properties due to surface and quantum confinement effects.^{5,6} Recent applications of nanocrystalline ZnO in solar cells,⁷ field effect transistors⁸ and nanogenerators⁹ make it a versatile material. In order to materialize these specific properties of ZnO nanomaterials in practical applications, it has been assumed that they are chemically stable in ambient atmosphere.⁶ Here we report that ZnO nanocrystals in powder-form (*not in liquid dispersion*) are

surprisingly ‘alive’ and active at room temperature. We observed that ZnO nanocrystals grow substantially at room temperature in ambient atmosphere, controlled by chemisorption of water vapor. In the liquid phase, the growth of ZnO nanocrystals is a well-studied phenomenon^{10–14} but the growth of ZnO nanocrystals that is described here, is in powder form and at room temperature. Additionally, the kinetics of our ZnO nanocrystals is different from the liquid phase, indicating a different growth mechanism.

Experimental Section

ZnO nanocrystals were synthesized in a hot wall reactor by chemical vapor synthesis.¹⁵ Details of the synthesis setup are reported elsewhere.¹⁶ A bubbler filled with diethylzinc (Strem, 95%) was used as a precursor delivery system and the bubbler was placed in an oil bath to control its temperature. Helium (Air liquide 5.0) was bubbled through diethylzinc to transport it into the reactor. An alumina tube with an inner diameter of 1.9 cm and a length of 45 cm was used as hot wall reactor. Oxygen (Air liquide 4.5) was used as oxygen source and was mixed with diethylzinc vapor just before the reactor to prevent preliminary oxidation of diethylzinc. The flow rates of oxygen and helium were controlled by mass flow controllers. Hot wall reactor temperatures of 1073 and 1173 K were used for the synthesis of ZnO nanocrystals producing initial average crystallite sizes of 11.7(3) nm and 18.3(1) nm, respectively. Corresponding flow rates of diethylzinc

*Corresponding Author. Phone: +49-203-379-4446. Fax: +49-203-379-4453. E-mail: markus.winterer@uni-due.de.

- (1) Liao, L.; Lu, H. B.; Li, J. C.; He, H.; Wang, D. F.; Fu, D. J.; Liu, C. *J. Phys. Chem. C* **2007**, 111, 1900–1903.
- (2) Kwak, G.; Yong, K. *J. Phys. Chem. C* **2008**, 112, 3036–3041.
- (3) Tsukazaki, A.; Ohtomo, A.; Onuma, T.; Ohtani, M.; Makino, T.; Sumiya, M.; Ohtani, K.; Chichibu, S. F.; Fuke, S.; Segawa, Y.; Ohno, H.; Koinuma, H.; Kawasaki, M. *Nat. Mater.* **2005**, 4, 42–46.
- (4) Wang, R.; Sleight, A. W.; Cleary, D. *Chem. Mater.* **1996**, 8, 433–439.
- (5) Wang, Z. L. *J. Phys.: Condens. Matter.* **2004**, 16, R829–R858.
- (6) Djurisic, A. B.; Leung, Y. H. *Small* **2006**, 2, 944–961.
- (7) Law, M.; Greene, L. E.; Johnson, J. C.; Saykally, R.; Yang, P. *Nat. Mater.* **2005**, 4, 455–459.
- (8) Suh, D.; Lee, S. Y.; Hyung, J. H.; Kim, T. H.; Lee, S. K. *J. Phys. Chem. C* **2008**, 112, 1276–1281.
- (9) Wang, X. D.; Song, J. H.; Liu, J.; Wang, Z. L. *Science* **2007**, 316, 102–105.

- (10) Viswanatha, R.; Amenitsch, H.; Sarma, D. D. *J. Am. Chem. Soc.* **2007**, 129, 4470–4475.
- (11) Viswanatha, R.; Santra, P. K.; Dasgupta, C.; Sarma, D. D. *Phys. Rev. L.* **2007**, 98, 255501.
- (12) Wong, E. M.; Bonevich, J. E.; Searson, P. C. *J. Phys. Chem. B* **1998**, 102, 7770–7775.
- (13) Meulenkaamp, E. A. *J. Phys. Chem. B* **1998**, 102, 5566–5572.
- (14) Li, Z.; Shkilnyy, A.; Taubert, A. *Cryst. Growth Des.* **2008**, 8, 4526–4532.
- (15) Winterer, M. *Nanocrystalline Ceramics—Synthesis and Structure*; Springer: New York, 2002.
- (16) Ali, M.; Friedenberger, N.; Spasova, M.; Winterer, M. *Chem. Vap. Deposition*, **2009**, 15, 192–198.

were 1.70×10^{-5} mol/sec and 3.96×10^{-5} mol/sec. The absolute pressure of the system was measured by a Baratron gauge and maintained at 2000 Pa for both syntheses using of a butterfly valve. ZnO nanocrystals, generated inside the reactor, were transported by the gas stream to the particle collector, where they were separated from the gas stream by thermophoresis.

The crystal structure and phase composition of the ZnO powders were determined by X-ray diffraction (XRD) using a PANalytical X-ray diffractometer (X'Pert PRO) using Ni-filtered Cu K α (1.54 Å) radiation produced by a Cu-tube at 40 kV and 40 mA and detected by an X'Celerator detector. The diffraction data were collected with a step size of 0.0084° and a scan speed of $0.021^\circ/\text{sec}$. The diffraction data ($2\theta = 20\text{--}120^\circ$) were analyzed to get the crystallite size by Rietveld refinement using the program MAUD.¹⁷ The background was fitted by a six parameters polynomial. Parameters characterizing the instrumental resolution were obtained from the LaB₆ standard material (NIST, 660a). The crystallite size, the rms microstrain, lattice constants, as well as stacking fault and twin fault probabilities and the temperature-factor were used as fitting parameters. The value of the temperature-factor (isotropic) for zinc and oxygen atoms were kept equal to each other and this value turned out to be in the range of 0.63–0.79 (Å).² The zinc and oxygen occupancies were fixed at unity as their variations generated inconsistent results. The details of the Rietveld refinement are discussed elsewhere.¹⁶ Refinements without including faults showed systematic deviations in the residual signal which could only be improved by including stacking faults in *c*-direction and {10 $\bar{1}2$ } twin faults. For transmission electron microscope (TEM) measurements the samples were thermophoretically deposited on a carbon-coated copper TEM grid directly from the gas flow at the exit of the reactor where the TEM grid was injected perpendicular to the gas flow and taken out after a deposition time of one second. A Philips CM12 twin microscope (accelerating voltage of 120 kV) with a LaB₆ cathode was used for TEM investigations. Around 500–1000 particles were analyzed to determine the size distribution of the samples. The mean particles size and geometrical standard deviation were calculated by fitting the size distribution with a log-normal-distribution function. The specific surface area of ZnO nanocrystals was measured using a nitrogen sorption instrument (Autosorb 1C Quantachrome). Before the adsorption measurement, ZnO nanocrystals were degassed in vacuum at 423 K for 2 h to remove any physisorbed gases. Diffuse reflectance infrared Fourier transform (DRIFT) spectra of ZnO nanocrystals (powder) were measured by Bruker IFS66v/S spectrometer. The weight percentages of carbon and hydrogen, determined by chemical analysis, are 0.58% and 0.27%, respectively for ZnO nanocrystals with starting crystallite size of 11.7(3) nm. For ZnO nanocrystals with starting crystallite size of 18.3(1) nm, corresponding percentages are 0.24% and 0.16%.

Results and Discussion

Figure 1 shows the XRD pattern of ZnO nanocrystals synthesized by chemical vapor synthesis. The first XRD of the sample was measured just after synthesis. The sample was then kept in an open bottle (transparent glass) at room temperature (294 K, air conditioned). Further measurements of XRD of the same sample were performed at regular time intervals. The decrease in line width of the

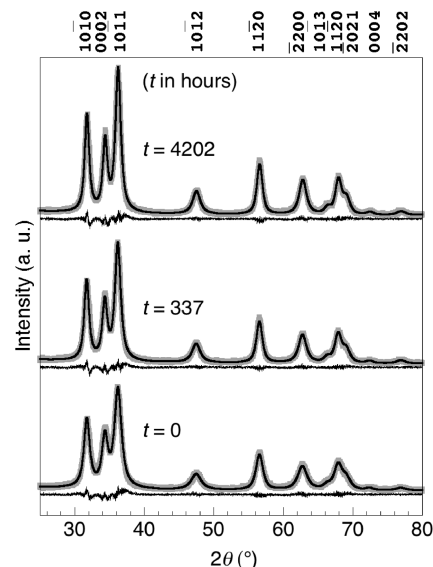


Figure 1. XRD of ZnO nanocrystals measured at different time intervals stored in ambient air. The Bragg reflections are getting sharper with time. Thick gray and thin black lines correspond to measured and Rietveld refined data, respectively. The residuals are shown just below the respective data.

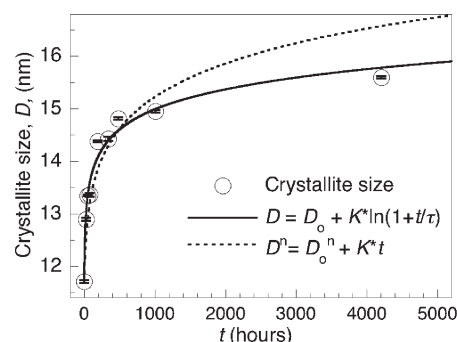


Figure 2. Crystallite size of ZnO nanocrystals plotted against growth time and fitted using a power law (broken curve, $K = 7 \times 10^{16} \pm 6 \times 10^{17}$ and $n = 17 \pm 3$) and a logarithmic law (solid curve, $K = 0.55 \pm 0.05$ and $t = 2.69 \pm 1.1$). The growth kinetics are best explained by a logarithmic rate law. The initial crystallite size, D_0 , is equal to 11.7(3) nm.

Bragg reflections corresponding to the Wurtzite phase of ZnO nanocrystals, indicates an increase in crystallite size with time (Figure 1). In order to get a clear understanding of the kinetics of this unexpected growth, the crystallite sizes of ZnO nanocrystals, determined by Rietveld refinement of XRD data at different time intervals, are plotted in Figure 2 (circles). If the same sample is kept in a similar glass bottle at room temperature (294 K, air conditioned) but covered with aluminum foil except for a few holes, the data overlap with the circles of Figure 2 (not shown here). This indicates that the growth of ZnO nanocrystals is not influenced by ambient light. Recently, the growth kinetics of ZnO nanocrystals in liquid phase systems, in the absence of organic capping agents, has been discussed elaborately^{10–12} and according to these reports the growth follows the equation

$$D^n = D_0^n + Kt \quad (1)$$

where K and n are constants, D is the particle diameter at time t , and D_0 is the particle diameter at $t = 0$. In this

(17) Lutterotti, L.; Matthies, S.; Wenk, H. R. IUCr: Newsletter of the CPD; International Union of Crystallography: Chester, England, 1999; 21, pp 14–15, Program available at <http://www.ing.unitn.it/~maud/>.

equation, the value of n depends on the growth mechanism. A value of n equal to 3 describes a diffusion-limited growth, controlled by the diffusion of the reactants toward the surface of ZnO nanocrystals.¹² This phenomenon is often termed Ostwald ripening. If n is equal to 2, the reaction of reactants with the surface of the particles controls the growth and any value between 2 and 3 causes a mixed growth.¹¹ Values of n in the range of 4–8 have also been observed for ZnO nanocrystals in the liquid phase and this slower growth-rate has been attributed to the unexpected role played by a part of reactants inhibiting the surface reactions.¹⁰ Similarly, the growth of micrometer-size ZnO by sintering at very high temperatures (> 1173 K) follows eq 1 with a growth exponent equal to three.¹⁸ This solid phase growth of micrometer-size ZnO takes place by lattice diffusion of Zn^{2+} ions. However, in our case it was not possible to get a reasonably good fit with eq 1 as shown in Figure 2. The broken line represents the fit with eq 1 where K and n were used as variables. A fit with eq 1 generated an unrealistic value of n equal to 17 ± 3 . We found that the growth of ZnO nanocrystals is fitted well with a logarithmic rate equation

$$D = D_0 + K \ln(1 + t/\tau) \quad (2)$$

where K and τ are constants and D_0 is defined as the diameter of ZnO nanocrystals just after the synthesis ($t = 0$).

The growth of oxide films on metal surfaces is a well-known phenomenon and it has been a topic of interest to metallurgists for a long time. For many metals, including zinc, the growth of an oxide film in atmospheric conditions follows logarithmic laws.¹⁹ Landsberg attributed chemisorption of atmospheric gases on the surface of metals as rate-limiting step for the growth of oxide films and derived the expression for chemisorption as²⁰

$$\frac{dq}{dt} = \frac{1}{b(t + \tau)} \quad (3)$$

where dq/dt is the amount of adsorbate chemisorbed per unit area per unit time after time t from the beginning of the exposure, b is the effective area over which active sites become invalidated by the adsorption of a single adsorbate molecule, and τ is a constant. The value of τ is equal to $1/\sigma N a b s_0$, where σ is a sticking coefficient, N is the number of adsorbate molecules colliding with the surface per unit area per unit time, a is the effective contact area between an adsorbate molecule and the surface upon collision, and S_0 is the number of active sites per unit area at $t = 0$. According to the kinetic theory of gases, the value of N is equal to $p/\sqrt{2\pi m k_B T}$, where p is the partial pressure of the adsorbate, m is the molecular mass of the adsorbate, k_B is the Boltzmann constant, and T is the gas temperature. Equation 3 is known in the field of chemisorption as Elovich equation.²¹ For the derivation of eq 3,

Landsberg assumed that the chemisorption of an adsorbate not only consumes the available active sites but also generates new active sites. Therefore, the value of b is the difference between the area of active sites consumed by the adsorption of one adsorbate molecule and the area of newly formed active sites generated by this adsorption. Landsberg's chemisorption kinetics was further extended by Cerofolini with an emphasis of surface reconstruction after chemisorption.²² Surface reconstruction has already been observed for ZnO.²³ Here the Landsberg chemisorption equation is extended to derive a logarithmic growth law for spherical ZnO nanocrystals.

As this unusual growth of ZnO nanocrystals occurs in ambient condition, atmospheric gases— H_2O , O_2 , and CO_2 —can be responsible for the growth. Room temperature application of ZnO as moisture sensor²⁴ and the observation of dissociative chemisorption of water even at low temperature (< 200 K),²⁵ compelled us to consider water as a potential cause of this unusual growth. Assuming ZnO nanocrystals are spherical in shape and at a particular instant of time, t , the radius of a ZnO nanocrystal is r . Active sites present on the surface of ZnO nanocrystals mediate the dissociative chemisorption of water molecules. Zinc atoms can migrate to react with these dissociatively chemisorbed water molecules. A possible growth mechanism is discussed later. In an infinitesimal time interval dt the number of water molecules chemisorbed per unit area on the surface of ZnO nanocrystal is dq , which leads to the formation of a new ZnO layer of thickness dr . The volume of this new shell of ZnO is $4\pi r^2 dr$. This volume is equal to the volume of a newly formed ZnO layer in time dt , which is $4\pi r^2 dq V_m f$, where V_m is the molecular volume of ZnO and f is defined as conversion-efficiency. A value of f equal to 1 means that the attachment of one molecule of water would lead to the formation of one molecule of ZnO. The volume balance of newly formed layers in time dt gives

$$\frac{dr}{dt} = \frac{dq}{dt} V_m f \quad (4)$$

Substituting the value of dq/dt from eq 3 into eq 4 and integrating it over r and t leads to eq 2, where the value of K is identified as $2V_m f/b$ and the initial growth rate of ZnO nanocrystals ($t = 0$) is given by

$$\frac{K}{\tau} = \frac{2V_m f \sigma a s_0 p}{\sqrt{2\pi m k_B T}} \quad (5)$$

In order to establish the influence of water vapor on the growth rate, ZnO nanocrystals were exposed to three different water vapor partial pressures. In the first case, granular CaCl_2 was partly filled in a glass bottle

(18) Senda, T.; Bradt, R. C. *J. Am. Ceram. Soc.* **1990**, 73, 106–114.

(19) Uhlig, H. H. *Acta Metallurgica* **1956**, 4, 541–554.

(20) Landsberg, P. T. *J. Chem. Phys.* **1955**, 23, 1079–1087.

(21) McIntock, I. S. *Nature* **1967**, 216, 1204–1205.

(22) Cerofolini, G. F. *J. Chem. Phys.* **2003**, 118, 10203–10211.

(23) Dulub, O.; Diebold, U.; Kresse, G. *Phys. Rev. Lett.* **2003**, 90, 016102.

(24) Zhang, Y.; Yu, K.; Jiang, D.; Zhu, Z.; Geng, H.; Luo, L. *Appl. Surf. Sci.* **2005**, 242, 212–217.

(25) Schiek, M.; Al-Shamery, K.; Kunat, M.; Traegerb, F.; Wöll, C. *Phys. Chem. Chem. Phys.* **2006**, 8, 1505–1512.

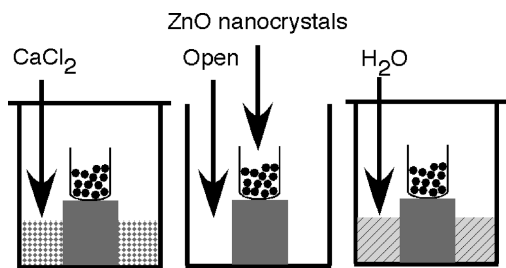


Figure 3. Freshly synthesized ZnO nanocrystals stored under three different conditions of varying water vapor pressures: over CaCl_2 , open to air, and over H_2O .

and a smaller beaker containing freshly synthesized ZnO nanocrystals was placed inside the glass bottle (Figure 3). The glass bottle was then closed with an airtight cap. For simplicity this bottle was labeled “ CaCl_2 -bottle”. CaCl_2 is a desiccant material that adsorbs moisture and decreases the moisture level of its closed surrounding to 1.5 mg per liter at 303 K.²⁶ In a second glass bottle, a second beaker containing the same ZnO nanocrystals was placed and the bottle was left open to air (labeled “open-bottle”). In a third glass bottle, instead of CaCl_2 , water was used and everything else was kept identical (labeled “ H_2O -bottle”). These three bottles were placed in an air-conditioned room at a fixed temperature of 294 K and a relative humidity of 55–60%. The approximate values of water vapor partial pressures in CaCl_2 -bottle, open-bottle, and H_2O -bottle are 200, 1500, and 2500 Pa,²⁶ respectively. XRD of ZnO nanocrystals, exposed to three different water vapor pressures, were measured at regular time intervals. For XRD measurements, samples were taken out of the bottles and after the measurements samples were placed back into their respective bottles. Figure 4a and b show the crystallite size of ZnO nanocrystals versus $\ln(1+t/\tau)$ for two different starting crystallite sizes—11.7(3) nm and 18.3(1) nm, respectively—exposed to three different water vapor pressures. The starting crystallite size, D_0 , is the crystallite size of the freshly prepared sample. The crystallite size follows a linear relationship as a function of $\ln(1+t/\tau)$, indicating a logarithmic growth rate of ZnO nanocrystals as predicted by eq 2, at different water vapor pressures. The slope of the curves is increasing with the water vapor pressure (Figure 4a and b). This implies an increase of the growth rate with increasing water vapor pressure. The initial growth rates of ZnO nanocrystals, K/τ , which is also increasing with increasing water vapor pressure (Figure 5), is consistent with eq 5. At a particular water vapor pressure, different values of K/τ for two different starting crystallite sizes are possibly due to the influence of starting crystallite size (or size-distribution) on any of these parameters V_m , σ , f , a , and s_0 . All these observations provide evidence that the growth rate of ZnO nanocrystals is influenced by the chemisorption of water vapor.

As the specific surface area of nanoparticles decreases with increasing particle-size, the growth of ZnO nanocrystals with time should also lead to a decrease in

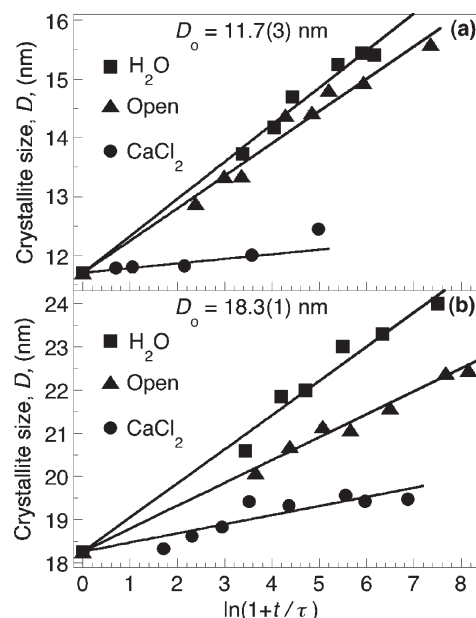


Figure 4. Logarithmic growth of ZnO nanocrystals of starting crystallite sizes of (a) 11.7(3) nm and (b) 18.3(1) nm. The error bars of crystallite sizes are smaller than the marker sizes.

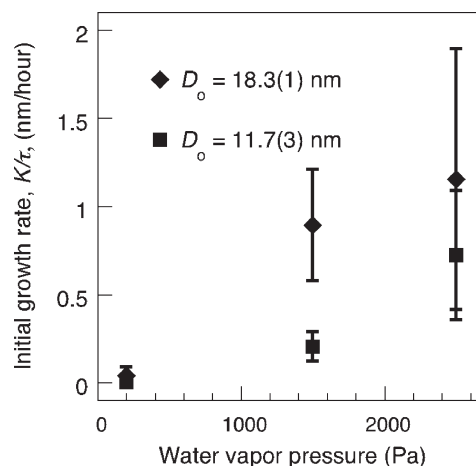


Figure 5. Initial growth rates, K/τ , increase with water vapor pressure, for both samples of ZnO nanocrystals.

their specific surface area. We observed that the specific surface area of ZnO nanocrystals with starting crystallite size, D_0 , of 11.7(3) nm and 18.3(1) nm, decreases with time as shown in Figure 6a and b, respectively. The specific surface area of freshly prepared ZnO nanocrystals is shown by a broken horizontal line. H_2O -bottle sample shows the highest decrease in specific surface area because of the highest water vapor pressure. A slight decrease in specific surface area of CaCl_2 -bottle sample is observed as the bottle had the lowest water vapor pressure. This water vapor pressure-dependent decrease in specific surface area of ZnO nanocrystals with time, justifies our observation that water vapor pressure influences the growth of ZnO nanocrystals. Figure 7a shows the TEM image of ZnO nanocrystals with an initial crystallite size of 18.3(1) nm. Particles were thermophoretically deposited on a TEM grid just at the exit of the synthesis reactor to avoid the dispersion of ZnO nanocrystals in any solvent.

(26) *Handbook of Chemistry and Physics*. 61st ed.; CRC Press: Boca Raton, FL, 1980–1981.

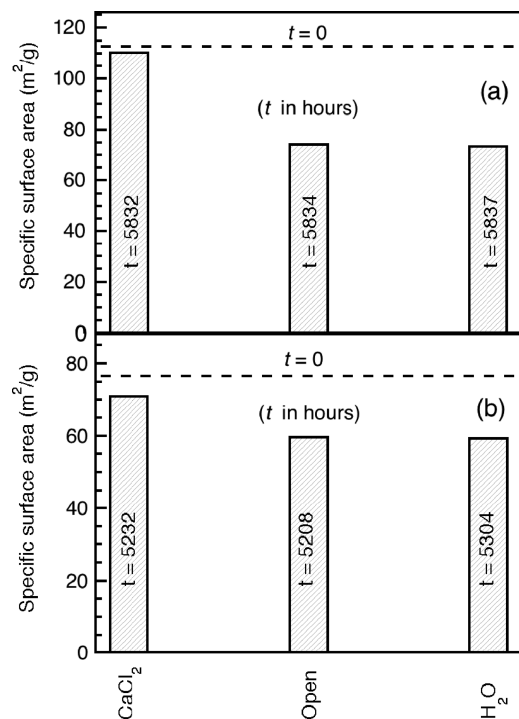


Figure 6. Decrease in specific surface area of ZnO nanocrystals with starting crystallite size, D_0 , of (a) 11.7(3) nm and (b) 18.3(1) nm. The decrease is the highest for the sample stored over H₂O, lowest for the sample stored over CaCl₂ and lies in between these two values for the sample that was kept open to ambient air. Broken-horizontal lines represent the specific surface areas of freshly prepared ZnO nanocrystals.

TEM images were taken at the day of synthesis. Figure 7b and c show initial particle size distributions of ZnO nanocrystals with initial crystallite sizes of 18.3(1) nm and 11.7(3) nm, respectively. We observed that ZnO nanocrystals are not stable in the electron beam and longer exposure leads to a sintering of ZnO nanocrystals. Therefore, the study of the growth of ZnO nanocrystals exclusively by TEM can be misleading.

Figure 8 shows DRIFT spectra of ZnO nanocrystals with initial crystallite size of 18.1(3) nm. The first DRIFT spectrum was measured 2 h after the synthesis. It is likely that the dissociation of water molecules has already started during that period of time. The presence of adsorbed water molecules on ZnO nanocrystals is evident by the peaks at 3447 cm⁻¹, 3557 cm⁻¹, 3619 cm⁻¹, 3639 cm⁻¹, 3660 cm⁻¹, and 3672 cm⁻¹. Broad peaks at 3447 cm⁻¹ and 3557 cm⁻¹ are assigned to hydroxyl groups formed via H₂O interaction with structural defects—steps, kinks, and edges—present on ZnO nanocrystals.²⁷ The strong and narrow peak at 3619 cm⁻¹ is assigned to hydroxyl groups on O-terminated ZnO (000 $\bar{1}$) surfaces, which are formed via dissociative adsorption of water on oxygen vacancy sites.²⁷ The bands at 3639 cm⁻¹, 3660 cm⁻¹, and 3672 cm⁻¹ are assigned to isolated hydroxyl groups and to hydroxyl groups interacting with coadsorbed water on mixed-terminated ZnO (10 $\bar{1}$ 0) surfaces, respectively.²⁷ Theoretically, it has been calculated that vibration frequency of OH (stretching) for protons at

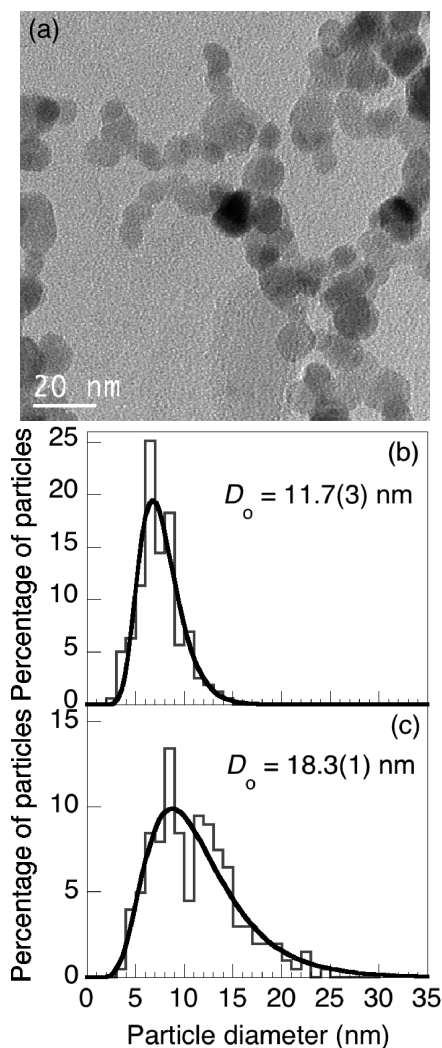


Figure 7. (a) TEM image of ZnO nanocrystals of starting crystallite size of 18.3(1) nm, showing agglomeration of the primary particles (nanocrystals). Particle size distribution of freshly synthesized ZnO nanocrystals with initial crystallite size, D_0 , of (b) 11.7(3) nm and (c) 18.3(1) nm.

bonding center appears at 3680 cm⁻¹.²⁸ Possibility of the OH vibration band at 3683 cm⁻¹ coming from protons, incorporated inside ZnO lattice, can not be excluded. Figure 8 also shows the DRIFT spectra of ZnO nanocrystals measured 4200 h after synthesis, which were stored under three different water vapor pressure conditions: in a CaCl₂-bottle, an open-bottle and a H₂O-bottle. After 4200 h, all the peaks are broadened and the broadening is largest for the highest water vapor pressure (H₂O-bottle) sample. The increase in broadening is possibly due to an increase in degree of interaction of hydroxyl groups with physisorbed water molecules.

Proposed Growth Mechanism. The dissociation of water molecules at oxygen vacancy sites, present on the surface of ZnO, has been reported earlier.^{27,29} ZnO is a material known for various intrinsic point defects.⁶ In chemical vapor synthesis, ZnO nanocrystals are synthesized under nonequilibrium conditions,¹⁵ which may

(27) Noei, H.; Qiu, H.; Wang, Y.; Löffler, E.; Wöll, C.; Muhler, M. *Phys. Chem. Chem. Phys.* **2008**, *10*, 7092–7097.

(28) Van de Walle, C. G. *Phys. Rev. Lett.* **2000**, *85*, 1012–1015.

(29) Kunat, M.; Girol, S. G.; Burghaus, U.; Wöll, C. *J. Phys. Chem. B* **2003**, *107*, 14350–14356.

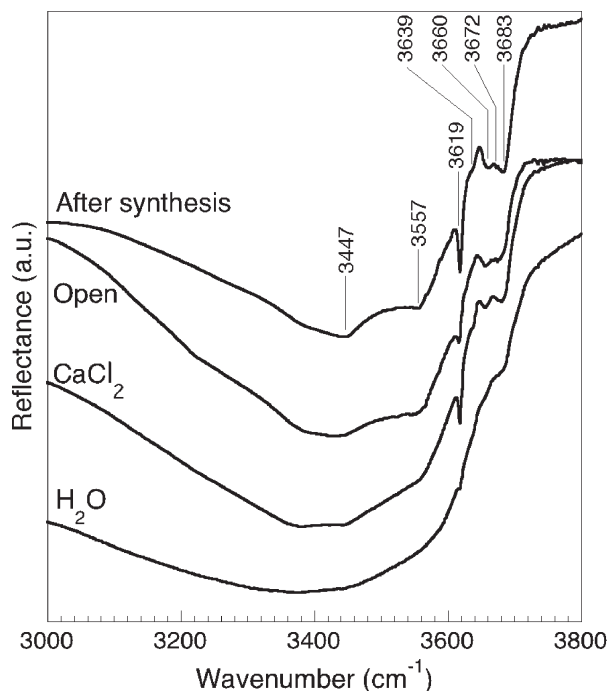
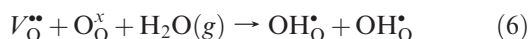
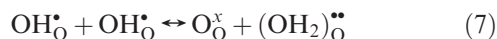


Figure 8. DRIFT spectra of ZnO nanocrystals with starting crystallite size of 18.3(1) nm, measured just after the synthesis and after 4200 h of the synthesis. On increasing the water vapor pressure, the peaks are broadened.

further increase the defect densities. Possibly, oxygen vacancies, $V_{\text{O}}^{\bullet\bullet}$, present on the surface of ZnO nanocrystals, behave as active sites for dissociative chemisorption of water. The doubly charged oxygen vacancy, $V_{\text{O}}^{\bullet\bullet}$, has a higher probability of formation as its formation enthalpy is lower compared to V_{O}^{\bullet} and V_{O}^{\times} .³⁰ The dissociation of one molecule of water can generate two hydroxyl groups,²⁹ as shown by eq 6 using the Kröger-Vink notation.



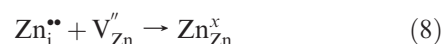
The presence of physisorbed water molecules on the surface of ZnO nanocrystals can not be excluded, as physisorption and chemisorption occur simultaneously. Protons, in form of surface hydroxyl groups, can be in equilibrium with neighboring hydroxyl groups at room temperature as shown by eq 7. This exchange equilibrium, with a low activation energy of 50 meV,³¹ occurs in the presence of chemisorbed water molecules in the neighborhood of hydroxyl groups.³²



Therefore, on the surface of ZnO nanocrystals hydroxyl groups and unprotonated surface oxygen coexist.

Self-diffusion of zinc in ZnO is believed to proceed through the migration of intrinsic defects and has been of fundamental as well as technological interest.^{33,34}

The highest mobility has been calculated for zinc interstitials followed by oxygen interstitials, zinc vacancies, and oxygen vacancies.³⁴ In fact, the threshold temperature for the migration of zinc interstitials is as low as 90–130 K.³⁴ A high specific surface area, no capping agents on the surface and the chain-like connectivity between ZnO nanocrystals (agglomeration shown in Figure 7a) in the samples investigated here can further enhance the transport of zinc interstitials. As the activation energy required for surface diffusion is smaller compared to bulk diffusion, the probability of zinc interstitials to migrate on the surface of ZnO nanocrystals is higher compared to bulk. Therefore, it is likely that zinc interstitials are mobile in ZnO nanocrystals even at room temperature. The encounter of zinc interstitials with zinc vacancies can lead to the formation of new ZnO layers, as shown by eq 8 and 9 together with eq 7.



Recently, the presence of protons in the ZnO lattice has been discussed as a cause of *n*-type conductivity in ZnO.^{28,35} Excess protons, generated by dissociation of water, can be incorporated into the subsurface lattice of ZnO nanocrystals, which can cause the neighboring zinc atom to relax outward by almost 40% of the bond length.²⁸ It is likely that this relaxed zinc atom, present on the surface, can switch to a neighboring interstitial site. The bare surface of ZnO nanocrystals can further enhance the relaxation of zinc atoms. Simultaneously, two hydrogen–oxygen bonds are generated,³⁵ which are possibly hydroxyl groups present on the surface of ZnO nanocrystals. This process can act as the source of zinc interstitials. As the ZnO nanocrystals are touching each other (Figure 7a) and are not monodisperse (Figures 7b and c), zinc interstitials present close to the surface of ZnO nanocrystals will try to migrate toward bigger particles or toward the neck to minimize the overall surface energy.³⁶ This may cause the merging of smaller particles into bigger ones and hence increases the average crystallite size of ZnO nanocrystals with time.

The overall effect of this proposed growth mechanism of ZnO nanocrystals is that the defect densities decrease with time, which is consistent with the decrease in rms microstrain—determined by Rietveld refinement of XRD data—with time (Figure 9a). The improvement in the degree of crystallinity—the ratio of coherent scattering to total scattering—with time indicates an overall decrease in defect density as well as a decrease in total surface area (Figure 5a). Twin and intrinsic stacking faults, as confirmed by HRTEM,¹⁶ in ZnO nanocrystals have been quantified by Rietveld refinement of XRD data in the

(30) Janotti, A.; Van de Walle, C. G. *Appl. Phys. Lett.* **2005**, *87*, 122102.

(31) Wöll, C. *Prog. Surf. Sci.* **2007**, *82*, 55–120.

(32) Meyer, B.; Marx, D.; Dulub, O.; Diebold, U.; Kunat, M.; Langenberg, D.; Wöll, C. *Angew. Chem., Int. Ed.* **2004**, *43*, 6642–6645.

(33) Gupta, T. K.; Carlson, W. G. *J. Mater. Sci.* **1985**, *20*, 3487–3500.

(34) Erhart, P.; Albe, K. *Appl. Phys. Lett.* **2006**, *88*, 201918.

(35) Lavrov, E. V.; Weber, J.; Börrnert, F.; Van de Walle, C. G.; Helbig, R. *Phys. Rev. B* **2002**, *66*, 165205.

(36) Rahaman, M. N. *Ceramic Processing and Sintering*; CRC Press: Boca Raton, FL, 2003.

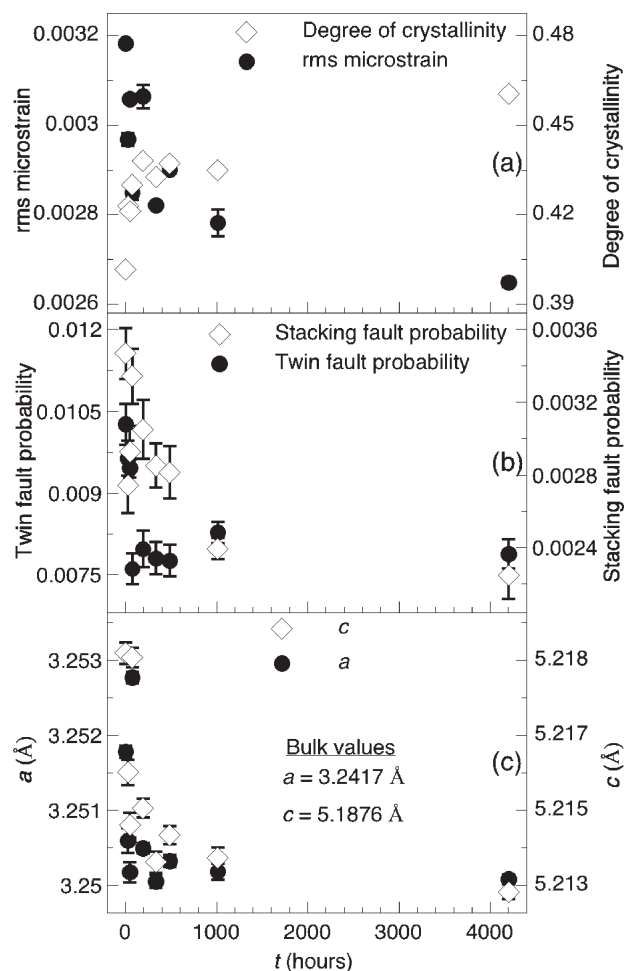


Figure 9. Influence of growth on the crystallinity of ZnO nanocrystals (initial crystallite size, D_0 , of 11.7(3) nm and stored in open-bottle). (a) Decrease in rms microstrain and improvement in degree of crystallinity of ZnO nanocrystals with growth time. (b) Decrease in twin and intrinsic stacking fault probabilities of ZnO nanocrystals with growth time. (c) Decrease in lattice parameters, a and c , of ZnO nanocrystals with growth time.

form of twin and intrinsic stacking faults probabilities. The fault probability is the fractional area of all closed-packed lattice planes, which are faulted. The decrease in twin and intrinsic stacking faults probabilities (Figure 9b) is correlated with an increase in crystallite size (increase in total area of lattice planes) with time. The possibility of water assisted etching of twin and intrinsic stacking faults due to their higher energies can not be ruled out.

The overall effect is that the defect density is decreasing with time indicating a self-healing nature of ZnO nanocrystals in ambient or water containing atmosphere. We also observed that the lattice parameters, a and c , of ZnO nanocrystals decrease with time (Figure 9c). The decrease in lattice parameters can be attributed to either the increase in crystallite size or the decrease in defect densities with time. For CeO_2 and ZnO nanocrystals it has been reported that the lattice parameters decrease with increasing the size.^{37–39} The competition between long-range Coulomb attraction and short-range repulsion creates an effective negative pressure in ionic nanocrystals, which causes the lattice to expand with decreasing the size.³⁷

Conclusions

So far nanocrystalline ZnO has enjoyed the status of a ‘stable and inert material’ in ambient atmosphere. Contradictorily, the presence of intrinsic defects, bare surfaces and chain-like connectivity make ZnO nanocrystals surprisingly ‘alive’ in ambient atmosphere at room temperature. This unexpected behavior of ZnO nanocrystals not only can have remarkable influences on their applications as catalysts and devices, especially sensors and transistors, but also can provide a better understanding of the surface of ZnO nanocrystals. The migration of ions in ZnO nanocrystals raises a serious question about the long-term reliability of devices fabricated with ZnO nanocrystals. The growth of ZnO nanocrystals and their self-healing behavior in ambient condition can open a new chapter in the field of sintering: water assisted low temperature sintering. It is likely that other nanoparticulate oxides, which have a higher reactivity toward water, show similar growth behavior.

Acknowledgment. The financial support of the German Research Foundation (DFG) through the Research Training Group: Nanotronics (1240) is gratefully acknowledged. We thank Anoop Gupta for TEM measurements, Axel Lorke for the use of the FTIR spectrometer and Dietrich Wolf for valuable discussions.

- (37) Perebeinos, V.; Chan, S. W.; Zhang, F. *Solid State Commun.* **2002**, *123*, 295–297.
- (38) Zhang, F.; Chan, S. W.; Spanier, J. E.; Apak, E.; Jin, Q.; Robinson, R. D.; Herman, I. P. *Appl. Phys. Lett.* **2002**, *80*, 127–129.
- (39) Li, J.; Kykyneshi, R.; Tate, J.; Sleight, A. W. *Solid State Sci.* **2007**, *9*, 613–618.